Electronic Supplementary Material (ESI) for Journal of Materials Chemistry A.

Supporting information

Modulation of Double-Network Hydrogels via Seeding Calcium Carbonate Microparticles for the Engineering of Ultrasensitive Wearable Sensors

Xiaohui Zhang,[a] Huimin Geng,[a] Xunhui Zhang,[a] Yaqing Liu,[a] Jingcheng Hao,*[a] and Jiwei Cui*[a,b]

[a]Key Laboratory of Colloid and Interface Chemistry of the Ministry of Education, School of Chemistry and Chemical Engineering, Shandong University, Jinan, Shandong 250100, China;

[b]State Key Laboratory of Microbial Technology, Shandong University, Qingdao, Shandong 266237, China

Email: jhao@sdu.edu.cn; jwcui@sdu.edu.cn

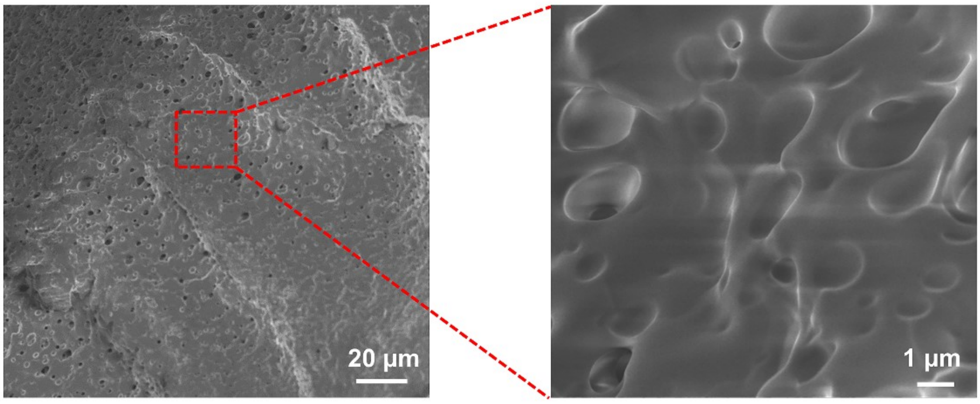

Fig. S1 SEM images of PAM hydrogels.

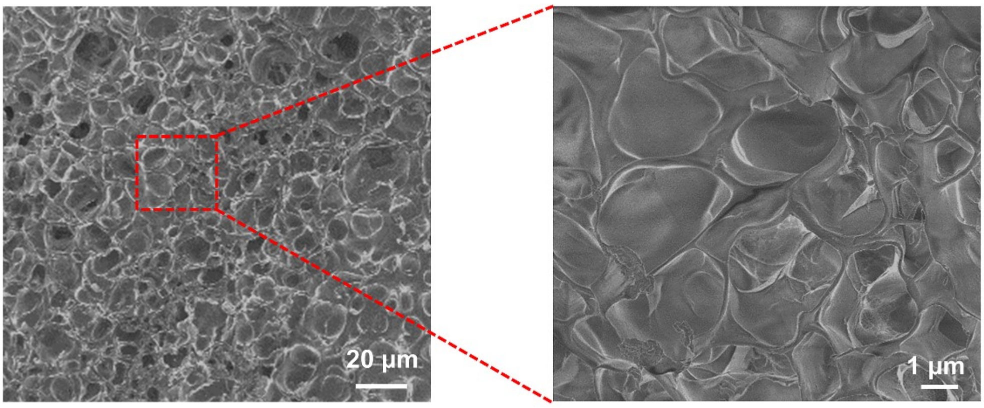

Fig. S2 SEM images of SA/PAM hydrogels.

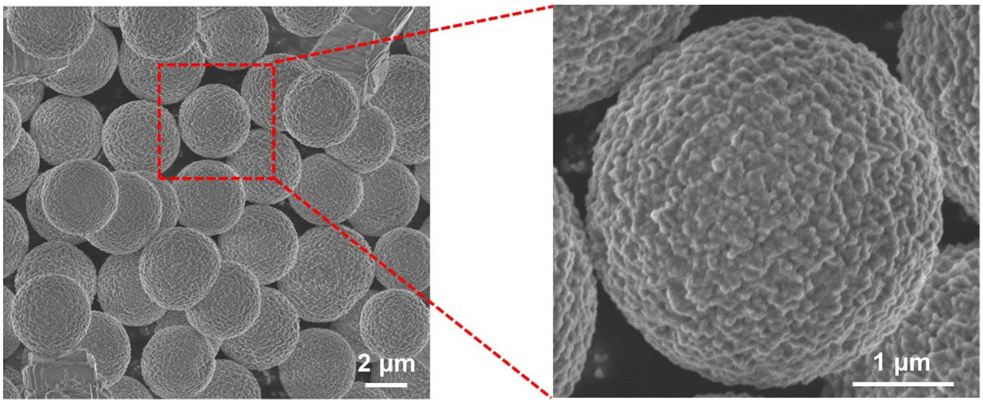

Fig. S3 SEM images of $CaCO_3$ microparticles.

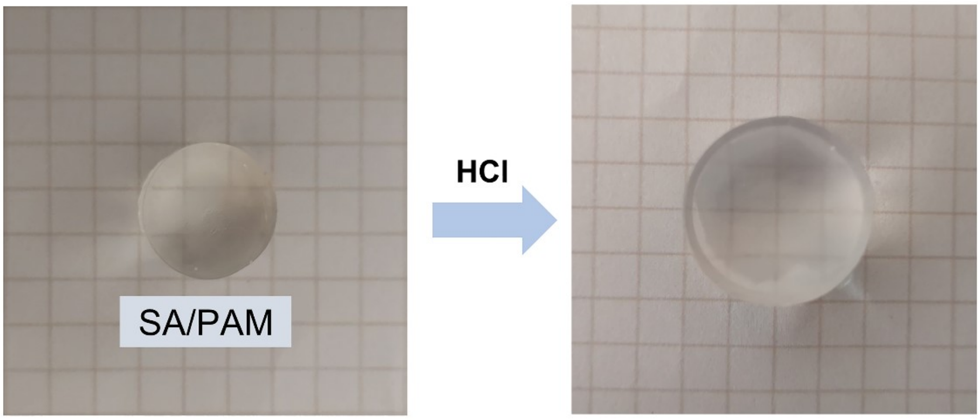

Fig. S4 Photographs of the SA/PAM hydrogel before and after the trigger with HCl.

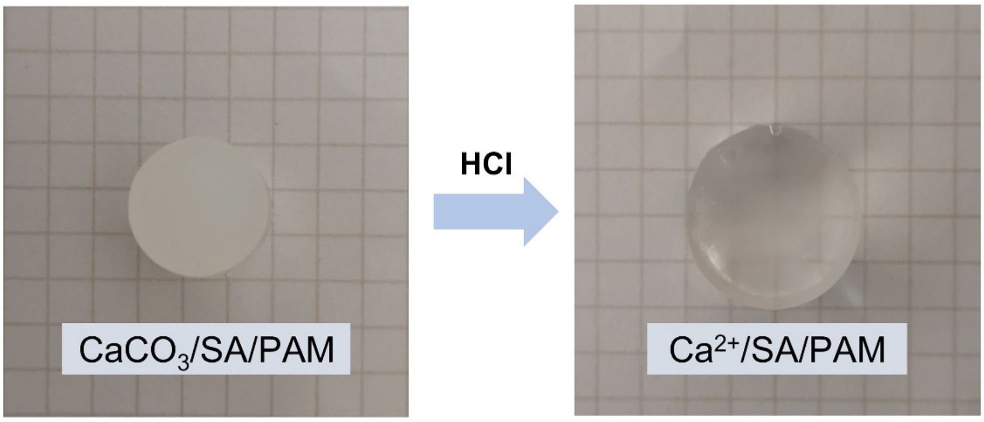

Fig. S5 Photographs of the $CaCO_3$/SA/PAM and Ca^{2+}/SA/PAM hydrogels after the trigger with HCl.

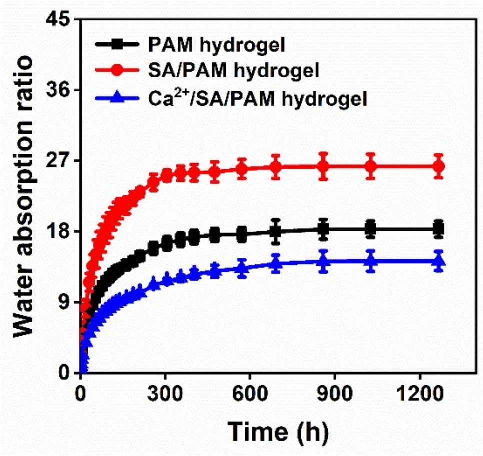

Fig. S6 Water absorption ratio of PAM hydrogels, SA/PAM hydrogels, and Ca^{2+}/SA/PAM DN hydrogels in water.

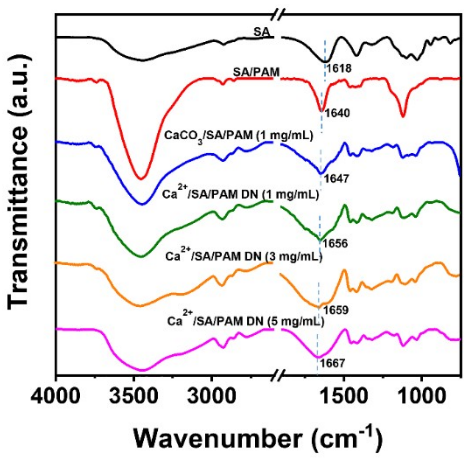

Fig. S7 FTIR spectra of SA powder, SA/PAM, $CaCO_3$/SA/PAM and Ca^{2+}/SA/PAM DN (at various concentrations of $CaCO_3$ microparticles, 1−5 mg mL^{-1}) hydrogels.

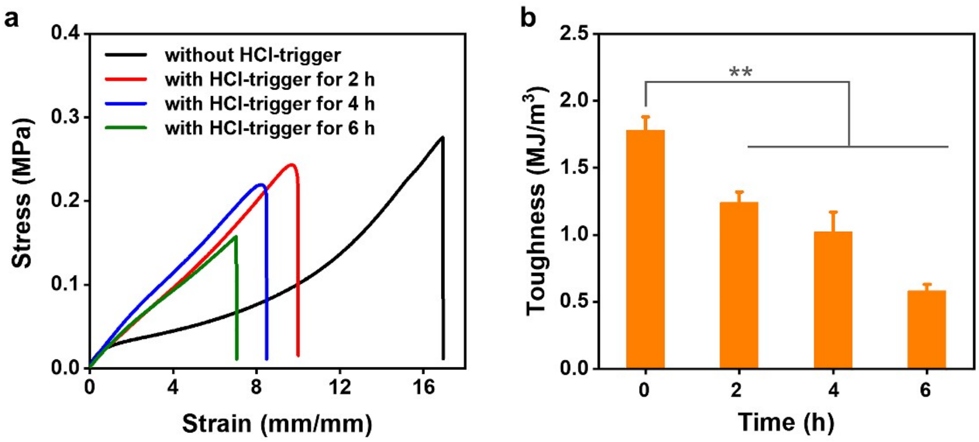

Fig. S8 (a) Tensile stress−strain curves and (b) corresponding toughness of SA/PAM hydrogels after trigger with HCl for different time.

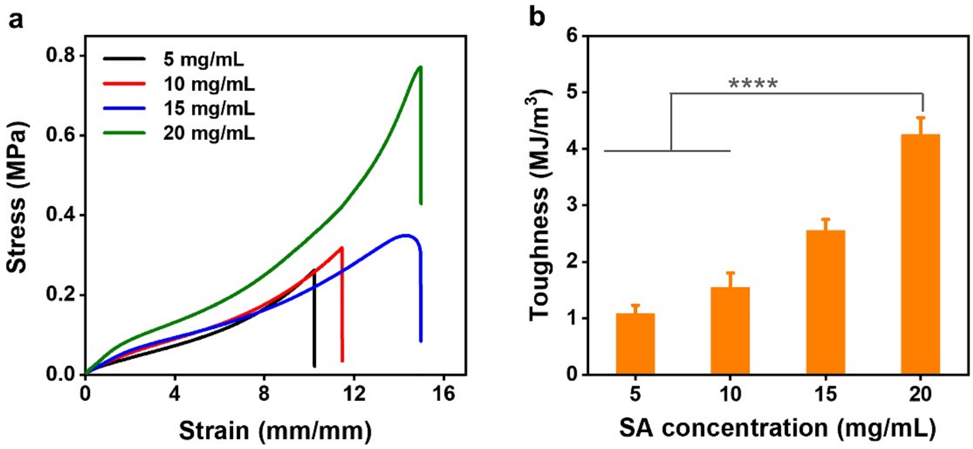

Fig. S9 (a) Tensile stress−strain curves and (b) corresponding toughness of Ca^{2+}/SA/PAM DN hydrogels at various concentrations of SA (the concentration of AM and MBAA were 320 and 0.2 mg mL^{-1}, respectively).

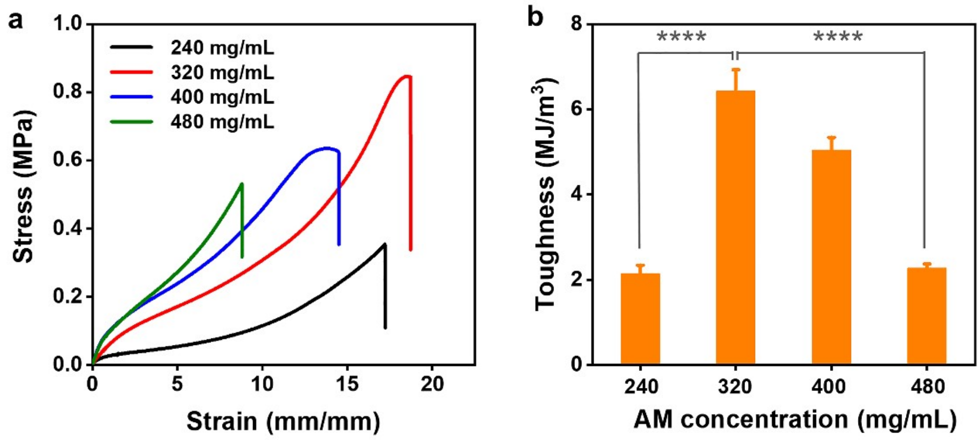

Fig. S10 (a) Tensile stress−strain curves and (b) corresponding toughness of Ca^{2+}/SA/PAM DN hydrogels at various concentrations of AM (the concentration of SA and MBAA were 20 and 0.2 mg mL^{-1}, respectively).

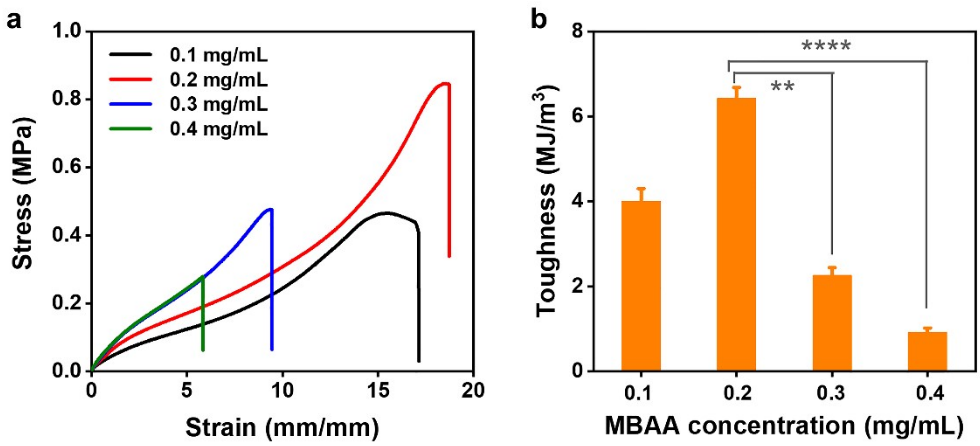

Fig. S11 (a) Tensile stress−strain curves and (b) corresponding toughness of Ca^{2+}/SA/PAM DN hydrogels at various concentrations of MBAA (the concentration of SA and AM were 20 and 320 mg mL^{-1}, respectively).

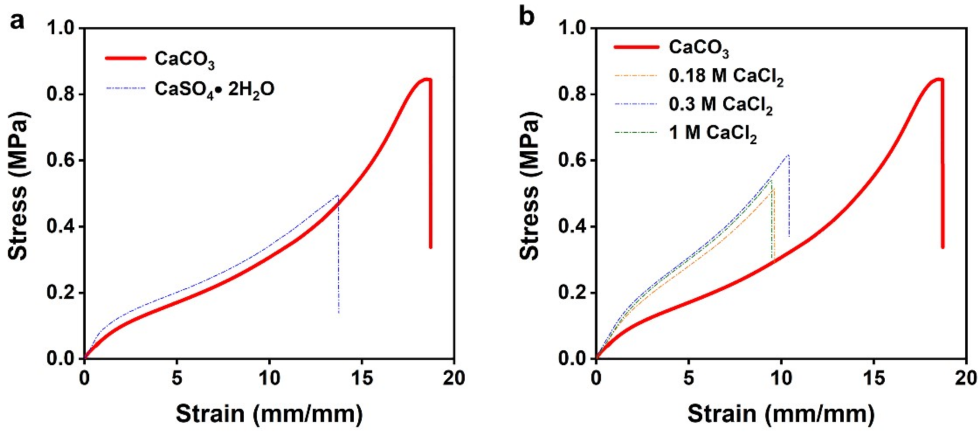

Fig. S12 (a) Comparison of Ca^{2+}/SA/PAM DN and $CaSO_4$/SA/PAM hydrogels with the same quantity of Ca^{2+}. (b) Comparison of Ca^{2+}/SA/PAM DN and $CaCl_2$/SA/PAM hydrogels at different concentrations of $CaCl_2$.

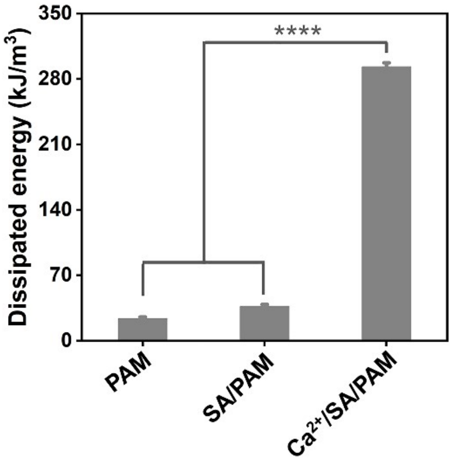

Fig. S13 The corresponding dissipated energy of PAM, SA/PAM, and Ca^{2+}/SA/PAM DN hydrogels under 500% strain by loading-unloading tests.

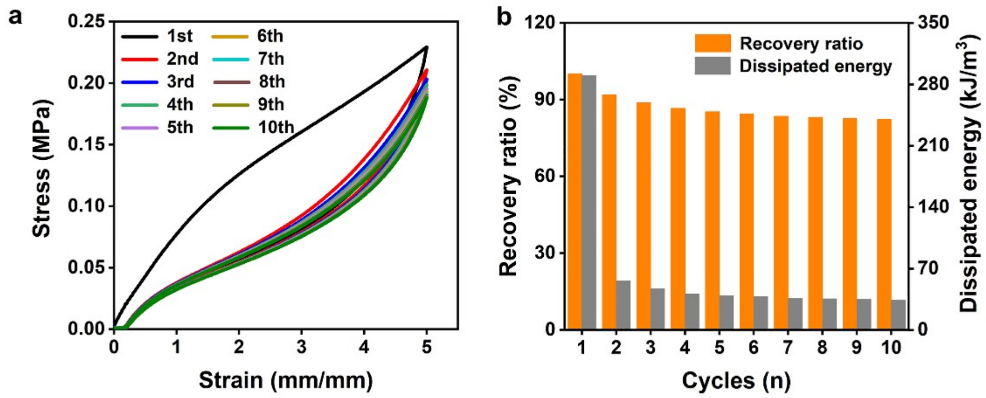

Fig. S14 (a) Stress-strain curves and (b) calculated recovery ratio and dissipated energy of Ca^{2+}/SA/PAM DN hydrogels with successive loading-unloading tests under 500% strain for 10 cycles.

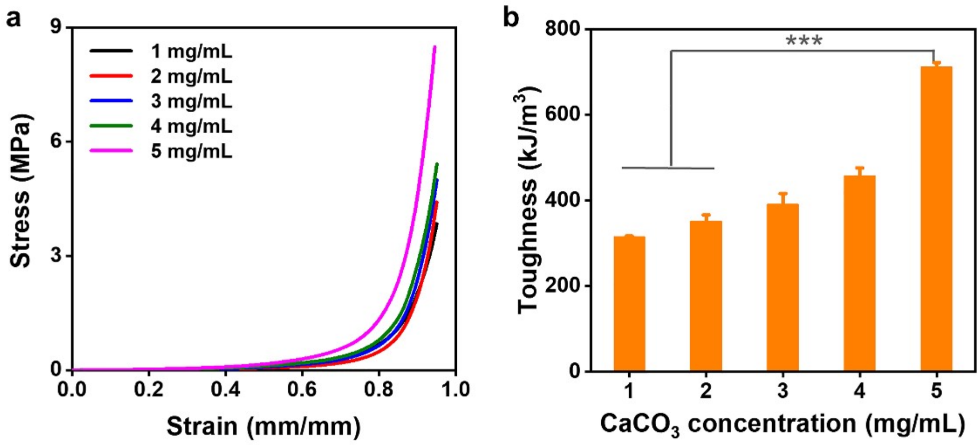

Fig. S15 (a) Stress−strain curves from compression tests and (b) toughness of Ca^{2+}/SA/PAM DN hydrogels at various concentrations of $CaCO_3$ microparticles.

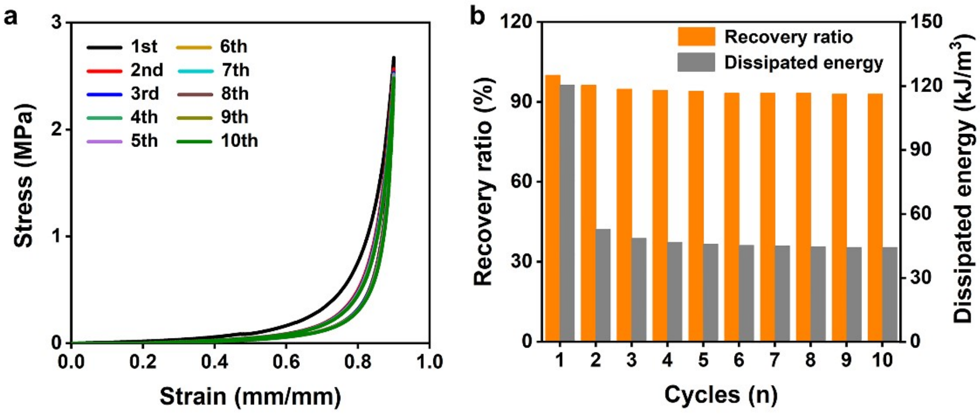

Fig. S16 (a) Loading−unloading tests and (b) calculated recovery ratio and dissipated energy of Ca^{2+}/SA/PAM DN hydrogels under 90% strain for 10 cycles without resting intervals.

Table S1. Summary of recent hydrogel-based flexible sensors.

Materials	Tensile property		Conductivity (S/m)	Gauge factor	Detection range ε (%)	Response time (ms)	References
	σ (MPa)	ε (%)					
CNF/CS/PAM	0.29	691	0.68	3.13	50-200	520	1
CNF/CS/P(AM-co-AA)	11	480	2.2	/	/	/	2
$ZnSO_4$/SA/PAM	0.15	700	3.24	/	/	/	3
NaCl/SA/PAM	0.65	2000	0.06	2.66	0.3-1800	/	4
F127-CHO/ MWCNT/P(AM-co-AEMA)/LiCl	0.15	1205	3.96	2.32	930	/	5
LMs/GelMA	0.15	150	/	48	150	50	6
Starch/PAM	0.06	135	0.13	0.98	/	/	7
PAA-r-BVIT/PEO	0.039	321	0.036	1.1	50-200	80	8
AP/P(AA-co-AM)/KCl	0.2	1089	0.17	8.82	/	100	9
LMA/PAM/PNIPAM/LiCl	0.96	1866	/	7.57	0.25-1500	197	10
HPMC-g-AN/AM-$ZnCl_2$	0.16	1730	1.54	0.94	/	/	11
PVA/P(SBMA-co-HEMA)	0.376	337	4.58	3.36	1-300	130	12
PAM/[EMIM]Cl	0.023	1160	3.87	6.78	50-800	/	13
CMC/PAM/LiCl	0.023	1363	/	3.15	100-500	360	14

CA/PAM/Li_2SO_4	0.225	2800	/	9.6	/	/	15
P(AM-APBA)/NaCl	0.21	1600	4.8	8	2.5-200	380	16
PAA/PANI NFs	0.036	991	/	18.28	5-268.9	/	17
PAA/ACC/Mxene	0.18	450	/	10.79	0.3-90	20	18
EDTANa_2Ca/SA/P(SBMA-co-HEMA)	0.294	975	0.39	3.26	/	/	19
MEA/AA/Graphene	0.175	1080	0.012	3.40	0.2-500	/	20
HLPs/P(AAm-co-LMA)/LiCl	1.37	2058	1.79	5.44	0.25-2000	151	21
PAM/CS-PA	0.150	1350	10.5	10.87	0.1-1000	291	22
Ca^{2+}/SA/PAM DN	**0.85**	**1850**	**0.85**	**8.91**	**0.03-1800**	**20**	**This work**

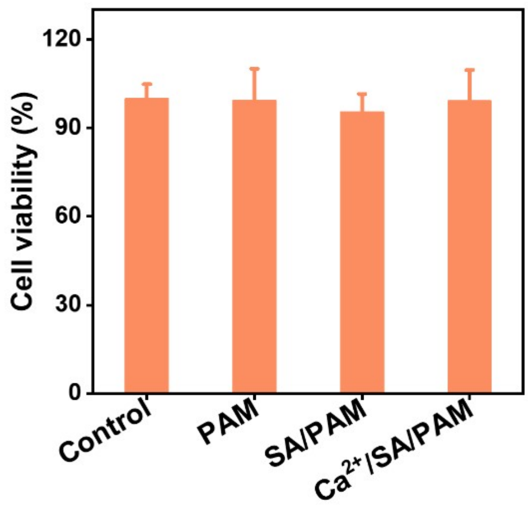

Fig. S17 Viability of NIH-3T3 cells after incubation with PAM, SA/PAM, or Ca^{2+}/SA/PAM hydrogel extracts for 24 h.

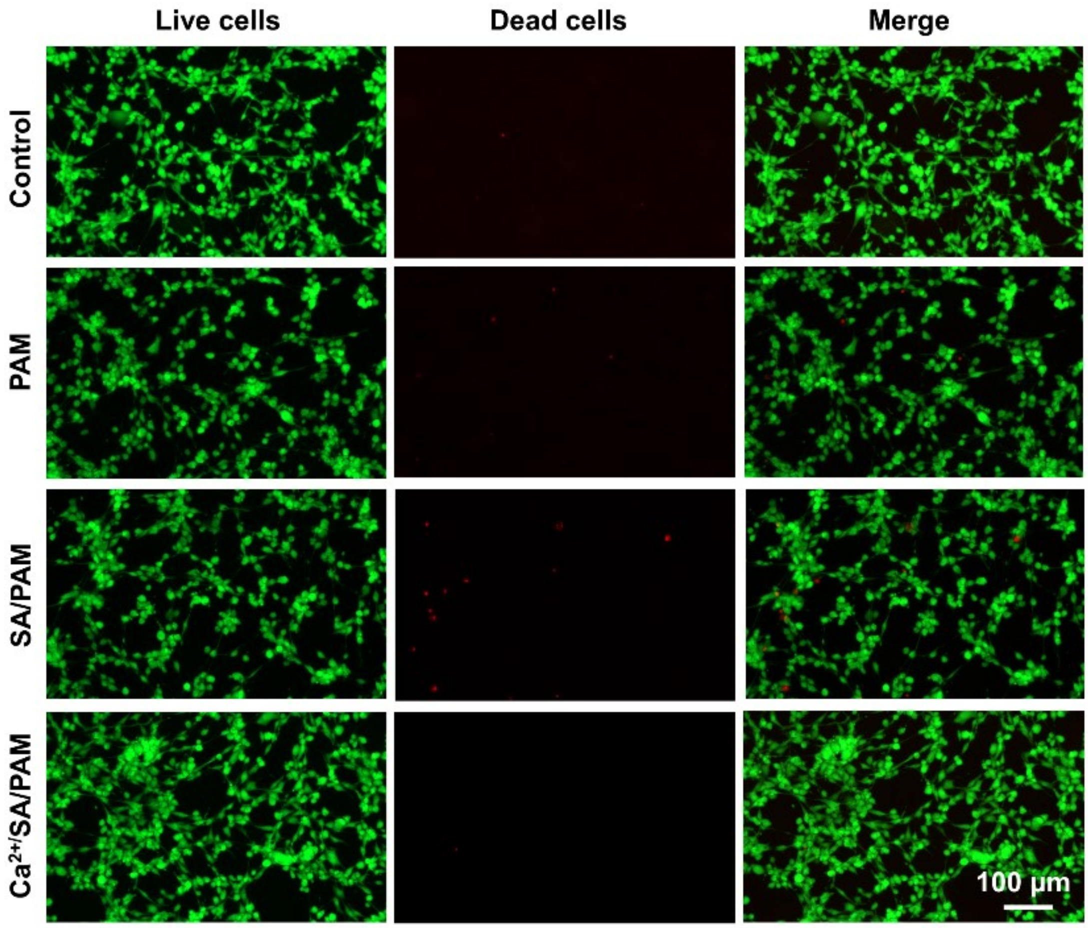

Fig. S18 Fluorescence microscopy images of live/dead NIH-3T3 cells after incubation with PAM, SA/PAM, or Ca^{2+}/SA/PAM hydrogel extracts for 24 h.

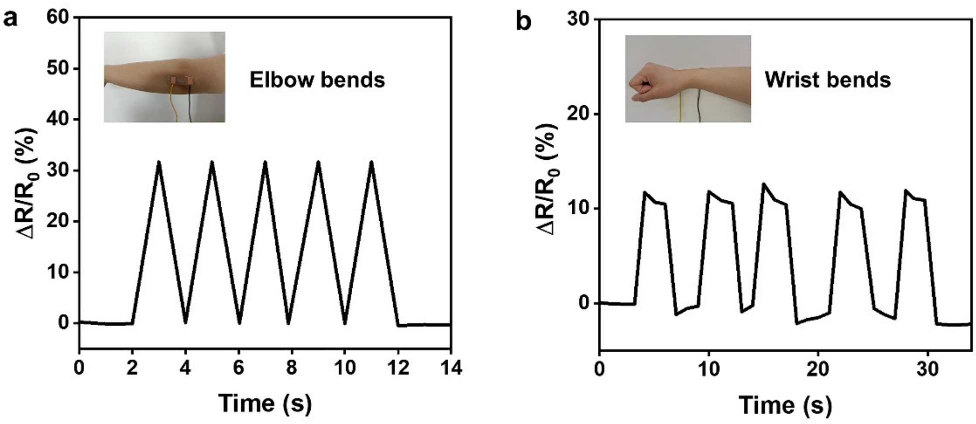

Fig. S19 Electrical resistance from the flexion and extension of (a) elbow and (b) wrist.

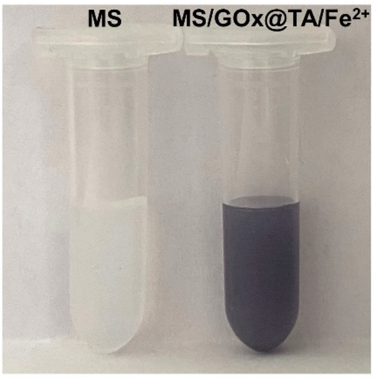

Fig. S20 Photographs of MS and MS/GOx@TA/Fe^{2+} NPs suspension.

Incubation of MS NPs with glucose oxidase (GOx), followed by coating with tannic acid (TA) and ferrous glycinate (Fe[Gly]$_2$), resulted in color changes of the MS suspensions, which indicated the successful preparation of the MS/GOx@TA/Fe^{2+} NPs.

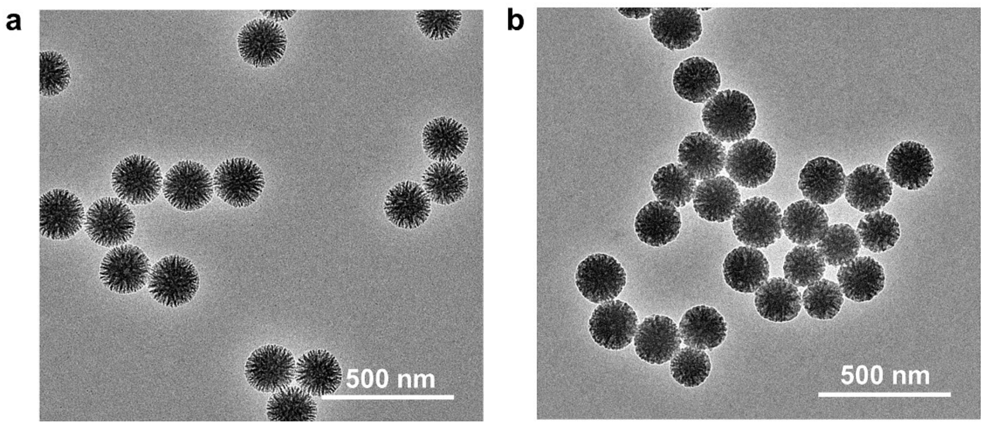

Fig. S21 TEM images of (a) MS NPs and (b) MS/GOx@TA/Fe^{2+} NPs with an average size of 175 nm.

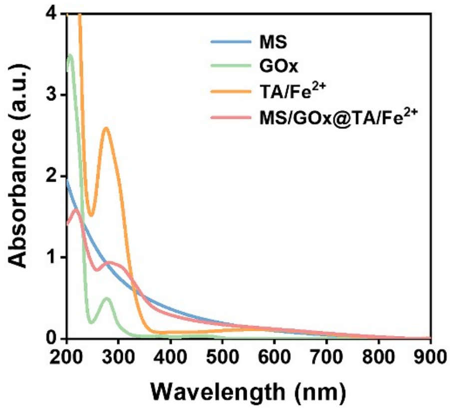

Fig. S22 UV-vis absorption spectra of MS NPs, GOx, TA/Fe^{2+} and $MS/GOx@TA/Fe^{2+}$ NPs, respectively.

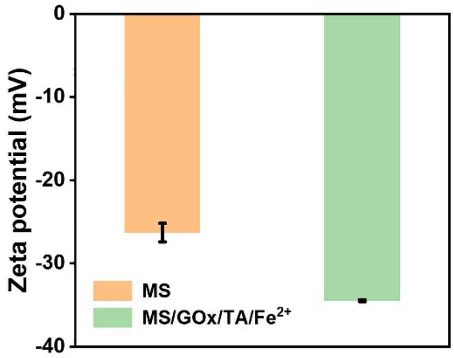

Fig. S23 Zeta potential of MS and MS/GOx@TA/Fe^{2+} NPs.

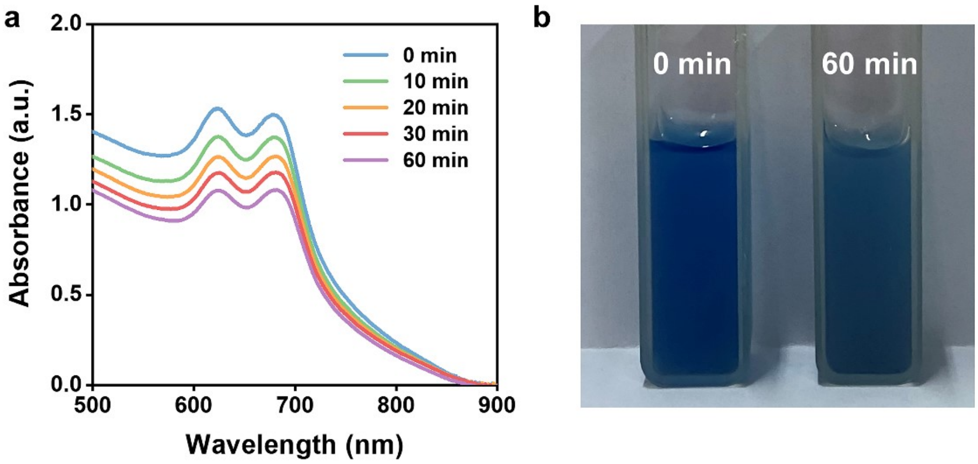

Fig. S24 UV-vis absorption spectra (a) and optical photograph (b) of solutions containing MB, glucose, and MS/GOx@TA/Fe^{2+} NPs at different time points.

References

1. J. Yu, Y. Feng, D. Sun, W. Ren, C. Shao and R. Sun, *ACS Appl. Mater. Interfaces*, 2022, **14**, 10886−10897.
2. L. Geng, S. Hu, M. Cui, J. Wu, A. Huang, S. Shi and X. Peng, *Carbohydr. Polym.*, 2021, **262**, 117936.
3. F. Mo, Y. Huang, Q. Li, Z. Wang, R. Jiang, W. Gai and C. Zhi, *Adv. Funct. Mater.*, 2021, **31**, 2010830.
4. X. Zhang, N. Sheng, L. Wang, Y. Tan, C. Liu, Y. Xia, Z. Nie and K. Sui, *Mater. Horiz.*, 2019, **6**, 326−333.
5. M. Wu, J. Chen, Y. Ma, B. Yan, M. Pan, Q. Peng, W. Wang, L. Han, J. Liu and H. Zeng, *J. Mater. Chem. A*, 2020, **8**, 24718−24733.
6. X. Yuan, P. Wu, Q. Gao, J. Xu, B. Guo and Y. He, *Mater. Horiz.*, 2022, **9**, 961−972.
7. S. Zeng, J. Zhang, G. Zu and J. Huang, *Carbohydr. Polym.*, 2021, **267**, 118198.
8. A. Wang, Y. Wang, B. Zhang, K. Wan, J. Zhu, J. Xu, C. Zhang and T. Liu, *Chem. Eng. J.*, 2021, **411**, 128506.
9. H. Zhou, J. Lai, B. Zheng, X. Jin, G. Zhao, H. Liu, W. Chen, A. Ma, X. Li and Y. Wu, *Adv. Funct. Mater.*, 2021, **32**, 2108423.
10. Q. Liang, X. Xia, X. Sun, D. Yu, X. Huang, G. Han, S. M. Mugo, W. Chen and Q. Zhang, *Adv. Sci.*, 2022, **9**, 2201059.
11. D. Chen, X. Zhao, X. Wei, J. Zhang, D. Wang, H. Lu and P. Jia, *ACS Appl. Mater. Interfaces*, 2020, **12**, 53247−53256.
12. J. Ren, Y. Liu, Z. Wang, S. Chen, Y. Ma, H. Wei and S. Lü, *Adv. Funct. Mater.*, 2021, **32**, 2107404.
13. M. Ma, Y. Shang, H. Shen, W. Li and Q. Wang, *Chem. Eng. J.*, 2021, **420**, 129865.
14. T. Zhu, Y. Cheng, C. Cao, J. Mao, L. Li, J. Huang, S. Gao, X. Dong, Z. Chen and Y. Lai, *Chem. Eng. J.*, 2020, **385**, 123912.
15. J. Chen, L. Zhang, Y. Tu, Q. Zhang, F. Peng, W. Zeng, M. Zhang and X. Tao, *Nano Energy*, 2021, **88**, 106272.
16. K. Xu, K. Shen, J. Yu, Y. Yang, Y. Wei, P. Lin, Q. Zhang, C. Xiao, Y. Zhang and Y. Cheng, *Chem. Mater.*, 2022, **34**, 3311−3322.

17. G. Ge, Y. Lu, X. Qu, W. Zhao, Y. Ren, W. Wang, Q. Wang, W. Huang and X. Dong, *ACS Nano*, 2020, **14**, 218−228.
18. X. Li, L. He, Y. Li, M. Chao, M. Li, P. Wan and L. Zhang, *ACS Nano*, 2021, **15**, 7765−7773.
19. H. Wei, Z. Wang, H. Zhang, Y. Huang, Z. Wang, Y. Zhou, B. B. Xu, S. Halila and J. Chen, *Chem. Mater.*, 2021, **33**, 6731−6742.
20. X. Liu, Q. Zhang and G. Gao, *ACS Nano*, 2020, **14**, 13709−13717.
21. S. Xia, Q. Zhang, S. Song, L. Duan and G. Gao, *Chem. Mater.*, 2019, **31**, 9522−9531.
22. Q. Zhang, X. Liu, J. Zhang, L. Duan and G. Gao, *J. Mater. Chem. A*, 2021, **9**, 22615–22625.